Title
Measuring longitudinal myelin water fraction in new multiple sclerosis lesions

Authors
Vargas, Wendy S
Monohan, Elizabeth
Pandya, Sneha
et al.

Publication Date
2015

DOI
10.1016/j.nicl.2015.09.003

Peer reviewed

NeuroImage: Clinical 9 (2015) 369–375

Contents lists available at ScienceDirect

NeuroImage: Clinical

journal homepage: www.elsevier.com/locate/ynicl

Measuring longitudinal myelin water fraction in new multiple sclerosis lesions

Wendy S. Vargas [a,*,1], Elizabeth Monohan [a,1,2], Sneha Pandya [d], Ashish Raj [b,d], Timothy Vartanian [a,b], Thanh D. Nguyen [d], Sandra M. Hurtado Rúa [c,2], Susan A. Gauthier [a,b,*]

[a] Department of Neurology, Weill Cornell Medical College, New York, NY, USA
[b] Feil Family Brain and Mind Research Institute, Weill Cornell Medical College, New York, NY, USA
[c] Department of Mathematics, Cleveland State University, Cleveland, OH
[d] Department of Radiology, Weill Cornell Medical College, New York, NY, USA

ARTICLE INFO

Article history:
Received 26 August 2015
Received in revised form 5 September 2015
Accepted 7 September 2015
Available online 12 September 2015

Keywords:
Multiple sclerosis
MRI
Myelin water fraction (MWF)
Acute lesion
Myelin

ABSTRACT

Objectives: Investigating the potential of myelin repair strategies in multiple sclerosis (MS) requires an understanding of myelin dynamics during lesion evolution. The objective of this study is to longitudinally measure myelin water fraction (MWF), an MRI biomarker of myelin, in new MS lesions and to identify factors that influence their subsequent myelin content.

Methods: Twenty-three MS patients were scanned with whole-brain Fast Acquisition with Spiral Trajectory and T2prep (FAST-T2) MWF mapping at baseline and median follow-up of 6 months. Eleven healthy controls (HC) confirmed the reproducibility of FAST-T2 in white matter regions of interests (ROIs) similar to a lesion size. A random-effect-model was implemented to determine the association between baseline clinical and lesion variables and the subsequent MWF.

Results: ROI-based measurements in HCs were highly correlated between scans [mean r = 0.893 (.764–.967)]. In MS patients, 38 gadolinium enhancing (Gd+) and 25 new non-enhancing (Gd−) T2 hyperintense lesions (5.7 months, ±3.8) were identified. Significant improvement in MWF was seen in Gd+ lesions (0.035 ± 0.029, $p < 0.001$) as compared to Gd− lesions (0.006 ± 0.017, $p = 0.065$). In the model, a higher baseline MWF ($p < 0.001$) and the presence of Gd ($p < 0.001$) were associated with higher subsequent MWF.

Conclusions: FAST T2 provides a clinically feasible method to quantify MWF in new MS lesions. The observed influence of baseline MWF, which represents a combined effect of both resolving edema and myelin change within acute lesions, suggests that the extent of initial inflammation impacts final myelin recovery.

1. Introduction

Multiple sclerosis (MS) is an immune-mediated disease targeting the myelin sheath and oligodendrocytes. Remyelination in response to injury within the central nervous system can be quite robust, however failure of this reparative process is widely accepted to occur in multiple sclerosis (Lassmann, 2014). Interestingly studies have demonstrated that levels of remyelination can occur in some patients (Patrikios et al., 2006; Patani et al., 2007) and factors leading to differential ability to repair are unknown. Primary reasons for overall remyelination failure in multiple sclerosis are unknown and are likely multi-factorial, (Franklin, 2002) however given the presence of oligodendrocyte progenitor cells in brains of multiple sclerosis patients (Chang et al., 2002) stimulation of these cells to enhance endogenous remyelination is considered the next frontier in therapeutic advancement for multiple sclerosis. Remyelination treatments would not only restore neuronal connectivity but would also function as a neuroprotective therapeutic strategy (Piaton et al., 2010). Understanding the variables that determine the extent of myelin loss within individual lesions will provide insight into potential therapeutic targets aimed at limiting residual damage and promoting repair.

Multi-compartment T2 relaxometry is an MR imaging technique in which a series of T2-weighted images at different echo times are obtained and the contribution of water associated with myelin and other tissue compartments can be differentiated using T2 decay curve analysis (MacKay et al., 2006). The relative contribution of the myelin water with respect to total water, is represented as myelin water fraction (MWF). Although T2 relaxometry is promising owing to its specificity for myelin, its clinical utility is currently impeded by a prohibitively long acquisition time, limited brain coverage, and challenging T2 data

* Corresponding author at: Department of Neurology, Multiple Sclerosis Center, Weill Cornell Medical College, Suite Y217, 1305 York Ave, New York, NY 10021, USA. Tel.: 646 962 3393; fax: 646 962 0390.
E-mail address: sag2015@med.cornell.edu (S.A. Gauthier).
[1] Authors contributed equally.
[2] Elizabeth Monohan, BS and Sandra M. Hurtado Rúa, PhD completed the statistical analysis.

http://dx.doi.org/10.1016/j.nicl.2015.09.003

analysis (Raj et al., 2014). To improve the data acquisition speed, our group has developed and optimized a signal-to-noise ratio efficient 3D spiral gradient echo sequence, (Nguyen et al., 2012) called Fast Acquisition with Spiral Trajectory and T2prep (FAST-T2), which enables rapid whole-brain MWF mapping within clinically feasible scan times at 3 T.

The goal of this study was to apply FAST-T2 to longitudinally quantify MWF after new MS lesion formation. We further extended our study to identify clinical and lesion characteristics that may influence resultant lesion MWF and provide a methodology to study the impact of future therapeutic targets on lesion myelin recovery.

2. Materials and methods

2.1. Patient population

This study is based on observational, prospectively collected data from a cohort of 23 patients with the diagnosis of either clinically isolated syndrome (CIS) or relapsing–remitting MS (RRMS) (Polman et al., 2005). Patients were selected from our ongoing database of over 500 clinical MRIs acquired with our FAST-T2 sequence. Patients were included in the study if a gadolinium-enhancing (Gd+) or non-enhancing (Gd−) new T2 lesion was identified on their baseline MRI and they had a follow-up scan within 2–12 months (mo). In addition, patients had at least one MRI within the previous year, which had the same conventional imaging protocol (3 T), to approximate lesion age. The following clinical data was collected: gender, age, disease duration (DD) from initial symptom, Expanded Disability Status Score (EDSS), disease subtype, steroid use at time of new lesion development, and change in medication at time of lesion development. Eleven healthy controls (HC) were recruited for test and retest MRI scans to confirm the reproducibility of our MWF quantification method within lesion-sized white matter (WM) regions of interests (ROIs). HC were scanned twice within the same imaging session. Institutional review board approval was obtained.

2.2. MRI data acquisition

Imaging was performed on a 3 Tesla GE scanner (HDxt 16.0) using a product 8-channel phased-array head coil. For anatomical scans, T1-weighted sagittal 3D BRAVO (1.2 mm isotropic) with (T1W + C) and without (T1W) gadolinium (Gd) contrast, T2-weighted (T2W) axial 2D ($0.5 \times 0.5 \times 3$ mm^3), and T2-FLAIR ($1.2 \times 0.6 \times 0.6$ mm^3) were used. Our whole-brain T2prep 3D spiral gradient echo imaging sequence, FAST-T2 ($1.2 \times 1.2 \times 5$ mm^3), has been previously described at 1.5 T (Nguyen et al., 2012). A modified BIR-4 adiabatic T2prep pulse (Soellinger et al., 2011) was developed to improve T2 weighting accuracy against the increased field inhomogeneity found at 3 T and enable whole brain coverage in only 10 min.

2.3. Fast-T2 post-processing

Our group has integrated a novel approach to deriving myelin maps from FAST-T2 data, which greatly improves robustness to noise, reduces spatial variations, and defines white matter fiber bundles in the brain (Raj et al., 2014; Kumar et al., 2012). Our approach to analyze the multiexponential T2 decay data method is called “Spatially constrained multi-Gaussian” algorithm and has been described elsewhere (Raj et al., 2014). This analysis method provides whole brain WM voxel-based MWF quantification.

2.4. Patient MWF registration and lesion identification

Subject’s T1W images where automatically processed using FreeSurfer’s longitudinal stream enabling us to register all sequences and all time points together for each patient (Reuter et al., 2012). The longitudinal stream creates an unbiased within-subject template space and uses information from this common space to create co-registered surface maps and parcellations for each time point. T2 FLAIR, T2W, and T1W + C images were linearly aligned onto the T1 FreeSurfer volume. Specific lesion ROIs were then manually defined based on the T2-FLAIR and T1W + C images on the baseline time point. The minimum volume of the lesion ROIs was 53 voxels and was easily visible on the MWF map. MWF maps were registered onto the T1 Freesurfer volume using a boundary based registration (BBR) method. Initially, the first echo of the T2-FAST sequence was registered to the T1W image using BBR. That resultant registration matrix was then applied to the processed MWF map. Each MWF map’s registration was quality checked prior to inclusion into the analysis (Greve and Fischl, 2009). The average lesion MWF for each time point was generated from the baseline lesion mask. All Gd+ lesions were new and had not been identified on prior MRI. All new Gd+ lesions had to demonstrate resolution of enhancement on follow-up scan. Fourteen of the 25 Gd− lesions, were new and enhancing on the previous MRI, therefore lesion ages could be accurately determined. The time between scans ranged from 1.5 to 8 months with a mean (SD) of 3 (3). The remaining 11 Gd− lesions were not seen on prior MRIs. Ages of these 11 Gd− lesions, where the date of enhancement was unknown, were roughly estimated by subtracting the date of the prior MRI from the date of the initial study MRI. All new Gd− lesions ages were estimated to be less than or equal to 12 months old. The time between scans ranged from 5 to 12 months with a mean (SD) of 9 (2).

2.5. Patient statistical analysis

A two-tailed paired t-test was utilized to explore longitudinal change in MWF within the lesions as well as comparing between different subtypes of lesions. A more sophisticated statistical model (a mixed-effect-model) was implemented to measure the effect of multiple covariates on final MWF within lesions while accounting for patient heterogeneity.

Mixed-effect-models are extensions of linear regression models for correlated data and are particularly useful in longitudinal studies (repeated measurements on same subject induce a correlation structure). Mixed-effect-models have several advantages over the classical repeated measure analysis: They naturally handle uneven spacing of repeated measurements, allow modeling flexible covariance structures and handle missing data. A mixed-effect-model has two components: fixed-effects and random-effects. In this context, fixed-effect terms can be seen as the traditional linear regression covariates while the random effects are associated with individual patient variability.

A mixed-effect-model was implemented with the final MWF at the lesion level as a response variable. This modeling approach was able to control for the random effect of patient heterogeneity and measure the fixed effects of the following individual covariates on the final MWF at the lesion level: baseline MWF (on initial MRI), lesion size, lesion age in months, interval follow-up, presence of gadolinium enhancement, DMT change after new lesion detection, intravenous (IV) solumedrol treatment after lesion detection, patient age, and estimated volume change. The best model was found using a back fitting procedure for fixed effects based on p-values.

2.6. Healthy control lesion-sized ROI reproducibility analysis

HC T1W images were automatically processed using FreeSurfer’s cross sectional stream (Fischl, 2012). The first echo of the spiral sequence was registered onto the T1W volume using boundary-based registration and that resulting matrix was then applied to the MWF map (Greve and Fischl, 2009). Ten patient lesion ROIs, representing varying sized lesions from the study patient cohort, were linearly aligned to the FreeSurfer average template and subsequently aligned onto the HC T1 FreeSurfer volumes (Fig. 1). Average MWF values were generated for the 10 WM lesion-sized ROIs for both test and retest HC scans. To measure lesion-sized ROI reproducibility, linear regression was performed using myelin test versus retest HC values at the ROI level and Pearson correlation

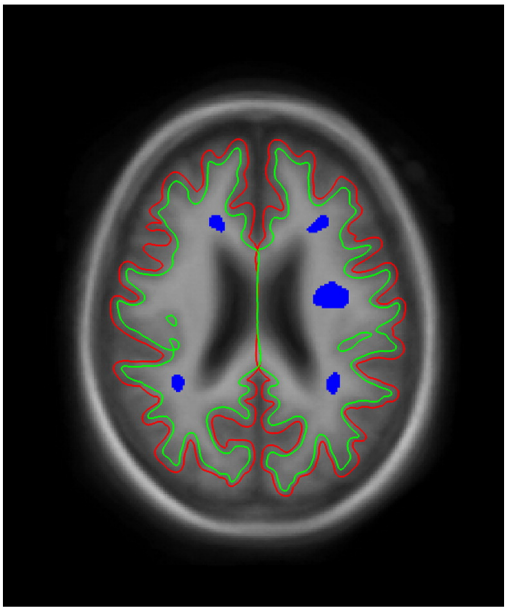

Fig. 1. Lesion-sized ROI examples. One slice example of the patient lesion ROIs (in blue) aligned onto the Freesurfer T1 average surface. Green line represents the estimated edge of the white matter surface. Red line represents that estimated edge of the pial surface.

coefficients were calculated between repeated scans for each HC. Lastly, a Bland–Altman plot was used to report the agreement between test and retest scans across all HC ROIs (Bland and Altman, 1999).

3. Results

3.1. FAST-T2 lesion-sized reproducibility

Given that measures of longitudinal changes in myelin content necessitate techniques that are consistent, precise and resistant to artifact and normal noise, we sought to first establish these characteristics from test–retest scans of healthy subjects. Ten WM ROIs were analyzed on each test and retest HC scan to confirm the reproducibility of FAST-T2. In total, 110 pairs of test–retest lesion-sized ROIs were created and 106 were ultimately used for reproducibility calculations (4 removed due to artifacts). The mean MWF of all ROI's combined was similar between both scans (0.160 ± 0.030 vs. 0.162 ± 0.029). Linear regression results in Fig. 2A represents the correlations between MWF values on test–retest HC scans, for all regions within all subjects combined. Pearson correlation coefficients demonstrated that MWF values were highly correlated between scans within individual HC [mean $r = 0.893$, (0.764–.967)]. The Bland–Altman plot revealed a negligible MWF bias with 95% limits of agreement of approximately ± 0.025 (Fig. 2B).

3.2. MWF within new MS lesions at baseline and follow-up

Twenty-three patients were identified from our ongoing database as having at least one new T2 hyperintense lesion. A total of 62 lesions (37 Gd+, 25 Gd−) were identified; multiple new lesions were present in 12 patients. The median age of Gd− lesions was 6 months (range 1.5–12) and median time to second MRI was 6 months for both lesion subtypes (Table 1). None of the 23 patients experienced an additional clinical relapse and the majority of patients (70%) had stable EDSS scores between MRI scans. Fig. 3A and B represents the change in MWF among

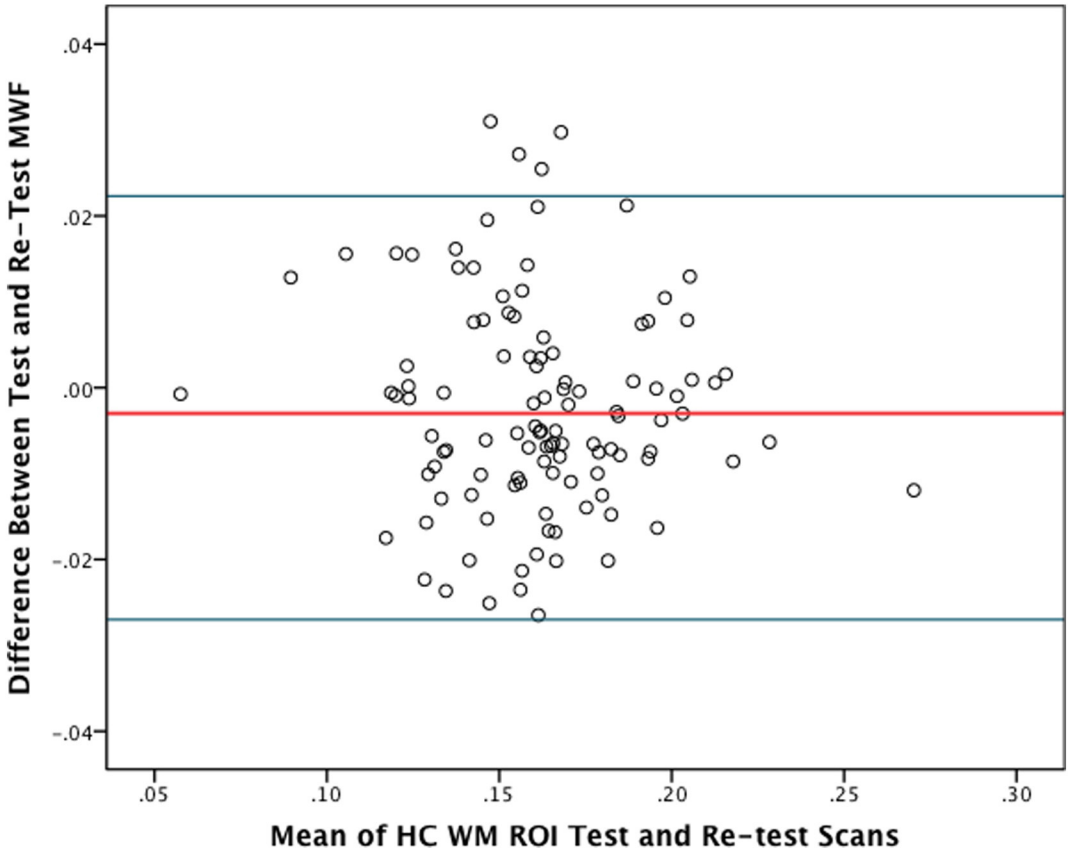

Fig. 2. HC lesion-sized ROI reproducibility. (A) Scatter plot of mean MWF measurements obtained from 10 WM ROIs in 11 HCs by repeated FAST-T2 scans. The linear regression line and its equation are shown. Both the linear correlation coefficient R squared and the slope of the regression line approach 1.0; indicating a strong agreement between test and retest scans. (B) Bland–Altman plot of the mean ROI measurements obtained from 10 WM ROIs in 11 HCs by test and retest FAST-T2 scans. The red line represents the mean difference between test and retest scans (0.003) and the blue lines indicate the 95% limits of agreement (−0.022–0.027).

Table 1
Patient and lesion characteristics.

Age of patient, mean years (±SD)	32.8 (7.9)
Female gender, n (%)	16 (66.7)
Disease duration, mean years (±SD)	5.3 (5.1)
EDSS, mean (±SD)	1.5 (1.3)
Patients with RRMS, n (%)	20 (86.9)
Patients with multiple lesions, n (%)	12 (50)
Number of Gd+ lesions, n (%)	37 (58.7)
Number of Gd(−) lesions, n (%)	25 (39.6)
Number of voxels in Gd+ lesions, mean (range)	416 (42–19,437)
Number of voxels in Gd(−) lesions, mean (range)	190 (53–627)
Age of Gd(−) lesions, mean (range)	6 (1.5–12)
Months between MRI 1 and MRI 2 for Gd+ lesions, median (range)	6 (3–12)
Months between MRI 1 and MRI 2 for Gd(−) lesions, median (range)	6 (2–12)
Average MWF on initial scan for all lesions, mean (±SD)	.065 (.035)
Enhancing lesions, mean (±SD)	.052 (.028)
Non-enhancing lesions, mean (±SD)	.081 (.033)
Average MWF on follow-up scan for all lesions, mean (±SD)	.089 (.036)
Enhancing lesions, mean (±SD)	.086 (.032)
Non-enhancing lesions, mean (±SD)	.088 (.037)

individual lesions within the different lesion subtypes: Gd+ versus Gd −. Gd− lesions showed a trend towards improvement (0.006 ± 0.017, $p = 0.065$) while Gd+ showed a greater magnitude of and statistically significant improvement (0.035 ± 0.029, $p < 0.001$). Given that MWF can be diluted due to an increase in extra-cellular water related to an acute inflammatory event, (Vavasour et al., 2009) the observed change within Gd+ lesions is likely a combination of both resolving edema and myelin recovery. This is demonstrated in Fig. 4, wherein there was a 212% relative improvement in MWF within an enhancing lesion, however partial resolution of the lesion on T2-FLAIR concurrently occurred and based upon previous studies, this suggests that resolution of edema is a contributing factor (Vavasour et al., 2009). Although baseline MWF was significantly different between Gd+ and Gd− lesions ($p < 0.001$), the MWF on follow-up scans (median follow-up time of 6 months) was similar ($p = 0.943$). These results suggest that if remyelination is occurring, the majority is likely to occur within the initial 6 months after lesion development, which is consistent with previous observations utilizing MTR to measure lesion recovery (Chen et al., 2008; Brown et al., 2013). However, two specific Gd− lesions (aged at 6 and 12 months) from different patients, demonstrated significant improvement. A hypothesis for this observation is that prolonged myelin recovery can occur in a subset of lesions. Only 1 Gd+ lesion demonstrated a true MWF decline, all other observed reductions were within the reproducibility bounds of the FAST-T2 method.

3.3. Variables associated with final lesion MWF

Two-tailed T-tests indicated that mean final MWF for both Gd+ (0.86 ± 0.032) and Gd− (0.88 ± 0.037) was significantly reduced ($p < 0.001$, $p < 0.001$, respectively) when compared to the overall mean MWF of all HC WM ROI derived from the initial test scan (0.160 ± 0.030). From this result, it was inferred that some level of myelin damage was detected in both lesion types at follow-up. We utilized a mixed effect model to examine association between several clinical and lesion characteristics and subsequent MWF for all lesions while controlling for multiple lesions per patient. The final model ($R^2 = 0.61$) included baseline MWF ($\beta = 0.8536$, $p < 0.001$) and the presence of Gd enhancement at baseline ($\beta = -0.0273$, $p = 0.0004$) as the only significant covariates. Lesion size, patient age and treatment interventions, such as intravenous steroid use, and baseline EDSS were not statistically significant. A lower baseline MWF, which is a combination of higher levels of edema (water) and lower myelin content, is associated with lower final MWF and suggests that more extensive acute inflammation leads to less myelin within lesions.

4. Discussion

Investigating the potential of myelin repair strategies in multiple sclerosis (MS) requires both a quantitative tool to measure myelin content in vivo and an understanding of natural dynamics of myelin repair/regeneration after initial lesion formation. The two imaging techniques most widely utilized to quantify myelin change are MWF and magnetization transfer ratio (MTR), (Chen et al., 2007) both of which provide an indirect measure of myelin. MTR has been more widely utilized given the wide availability of the sequence and simple reconstruction (Brown et al., 2013). In this study, we utilized FAST-T2 to describe MWF within two subtypes of new MS lesions (Gd+ and Gd− lesions). We chose to focus on multi-compartment T2 relaxometry, largely, because our group has developed a clinically feasible sequence and novel post-processing approach to minimize the typical noise present in MWF maps. In addition, we have devoted considerable effort to MWF given that the short T2 component of the T2 spectrum, representing myelin water, is felt to be more specific to

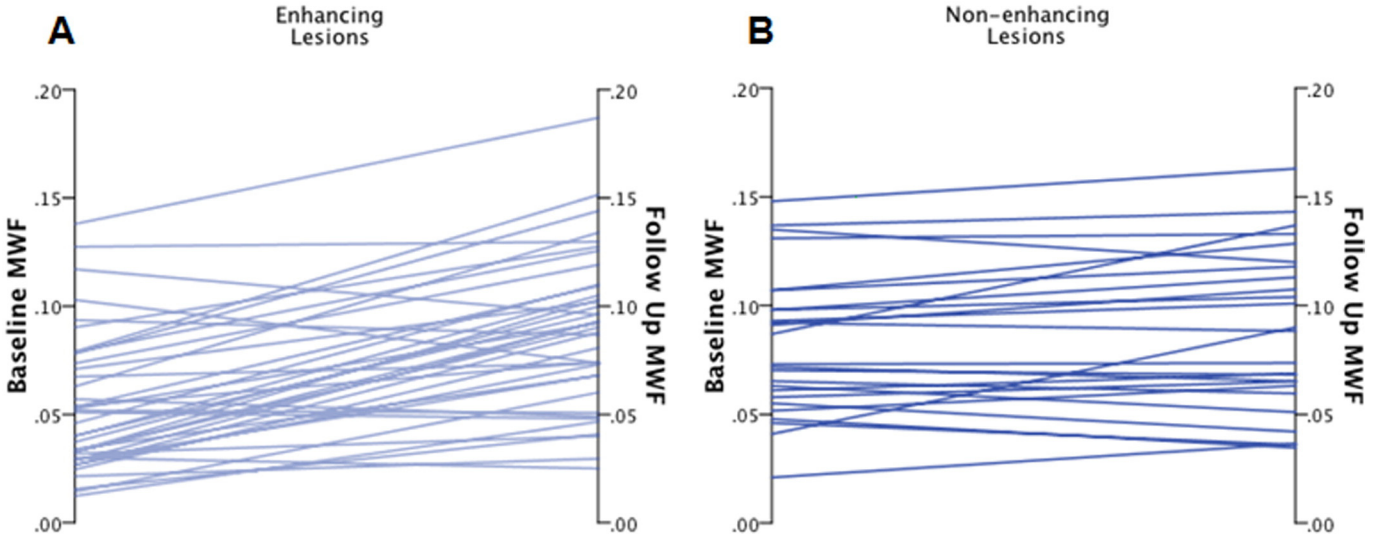

Fig. 3. MWF change in Gd+ and Gd− lesions.Trajectory of baseline and follow-up MWF values for (A) enhancing and (B) non-enhancing lesions. Enhancing lesions started at lower MWF values and had greater average change than non-enhancing lesions. Green lines: lesions that increased in MWF beyond our reproducibility threshold; red line: a lesion that decreased in MWF beyond our reproducibility threshold; gray lines: lesions that increased or decreased within our threshold.

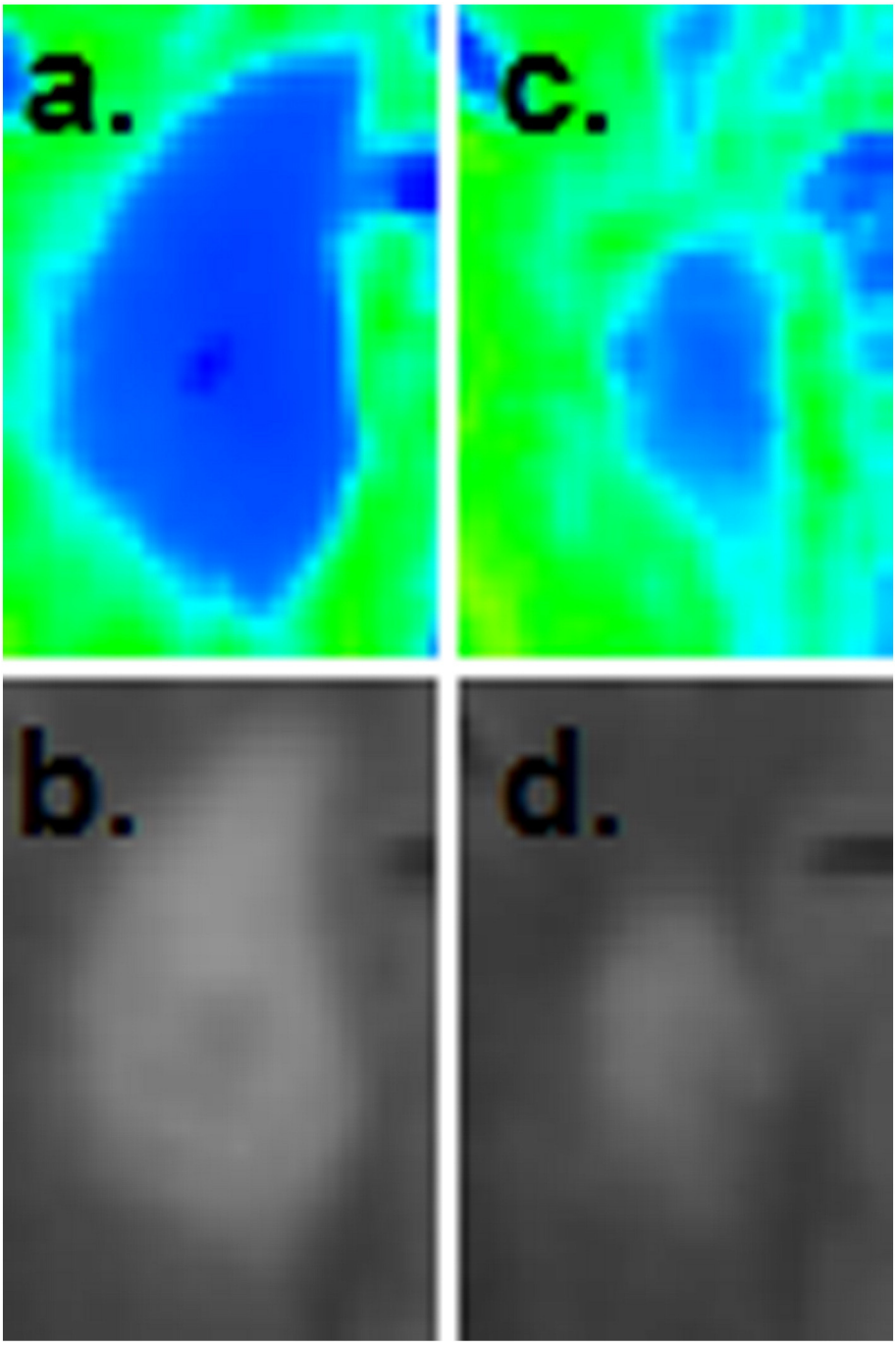

Fig. 4. An example of an enhancing lesion that demonstrated a large improvement in MWF. (A) Baseline T2-FLAIR image and the corresponding MWF map. (B) Follow up T2-FLAIR image and it's corresponding MWF map 6 months later (212% improvement). Partial resolution of the lesion can be appreciated on both the T2-FLAIR and MWF images (inset).

myelin as compared to MTR (Laule et al., 2007). MWF has been shown to highly correlate with histological myelin measurement in animal models (Gareau et al., 2000) and ex-vivo brain, (Laule et al., 2006; Laule et al., 2008) and has been applied to MS patients, (Laule et al., 2004) for which significant differences have been found when compared to controls (Kolind et al., 2012; Oh et al., 2006; Vavasou et al., 2006). In addition to our approach, there are a number of other investigators proposing sequences with the similar goal of clinically feasible whole brain myelin mapping (Neema et al., 2009; Prasloski et al., 2012; Oh et al., 2007; Deoni et al., 2008). In this study, we demonstrate that it is possible to implement longitudinal FAST-T2 mapping into a large cohort of over 500 patients, which allowed us to capture and present one of the largest study of MWF within acute MS lesions. Furthermore, we established that FAST-T2 is a reliable method to study MWF within lesions given that our reproducibility testing in HC is within the range of previous MWF studies (Meyers et al., 2009; Meyers et al., 2013).

We found that the most dynamic change occurred in new MS lesions having the presence of gadolinium on T1 post-weighted images, which we consider the younger of the two subtypes of lesions. Our results imply that lesions have the most potential to improve during the first 6 months after enhancement and stabilize during the second 6 months. Although we are unable to determine the precise timing of lesion formation, it has been accepted that the presence of gadolinium represents early stage lesions due to the breakdown of the blood brain barrier and is indicative of active inflammation within lesions (Cotton et al., 2003;

Blezer et al., 2007). Furthermore, we confirmed that all Gd+ lesions in this study were not present on previous MRI scans. Even though MWF measurement can be confounded by edema, it is likely that some of the change in Gd+ lesions is due to myelin repair, given that pathological studies showed that remyelination increases dramatically after the onset of demyelination in acute lesions (Prineas et al., 1993; Raine and Wu, 1993) and is consistent with previous MTR studies (Chen et al., 2008). We observed that the slightly older Gd− MS lesions were fairly quiescent, although improvement in MWF occurred within two lesions and thus raises the possibility that the temporal course of myelin repair may be prolonged in some lesions. In contrast to our study, which shows stability of the myelin signal in the majority of lesions >6 months of age, an MTR lesion study reported that the majority of lesions this age show progressive decline in the MTR signal, suggesting continued demyelination throughout the first year of lesion development (Chen et al., 2008). This divergence from our results may be reflective of MTR's sensitivity to other white matter microstructural changes, such as axonal loss (van Waesberghe et al., 1999) whereas MWF is specific for myelin (Laule et al., 2008).

MWF, given the nature of the fraction (myelin water/total water), is diluted with additional extra-cellular water and will likely overrepresent myelin recovery. Vavasor et al. demonstrated that an increase in water content (WC) occurred within acute lesions which was followed by subsequent resolution within the following months; this study provided evidence that WC must be taken into account while measuring MWF change in acute lesions (Vavasour et al., 2009; Laule et al., 2004). Given this limitation of MWF in Gd+ lesions, prediction of MWF change would not be appropriate nor would be an estimation of absolute myelin recovery in these early staged lesions. However, MWF as a *combined* measure of edema and demyelination provides a metric to represent the intensity of the initial demyelinating event. In our random effect model, we found that initial MWF was associated with subsequent MWF, thus more edema and demyelination during the acute inflammatory event influence the subsequent MWF value. From pathological studies, we know that within the acute phase of a new MS lesion, there are activated mononuclear cells, including lymphocytes, microglia, and macrophages which destroy myelin and to a variable degree, oligodendrocytes (Lassmann, 2011). If this highly inflammatory process is arrested at an early phase, plaques are partially remyelinated (Franklin and Ffrench-Constant, 2008). If instead, this inflammatory state persists, a variety of pro-inflammatory mediators are secreted, such as cytokines, reactive oxygen species, nitric oxide and glutamate, and these are able to induce further tissue damage and lead to failure of remyelination (Bitsch et al., 2000; Smith and Lassmann, 2002). Our work is in keeping with, but does not conclusively validate, the histopathological observations that inflammation may deleteriously impact remyelination potential. In addition, baseline MWF is predictive of follow-up MWF in Gd− lesions where, presumably, the MWF is less confounded by edema. This implies that even outside of the acute inflammatory event, baseline MWF is predictive of future MWF within lesions.

There are limitations to our study. Given the small sample size, limited duration of follow-up, and the estimated ages of Gd− lesions, we are not able to accurately determine the precise timing of MWF recovery within new lesions nor can we generalize our results to larger populations of MS patients. Importantly, we plan to further explore the dynamic changes of MWF in various aged lesions, compare MWF in T1 hypointense lesions to those that are T1 isointense, and expand our patient cohort in an attempt to make clinical correlations with MWF recovery. In addition, as discussed previously, changes in local tissue water in acute edematous lesions can confound MWF-based myelin quantification (Laule et al., 2004). It would be reasonable to postulate that the bulk of the dynamic change we observe in Gd+ lesions is due to inflammation resolution rather than remyelination. This limitation can be overcome by mapping absolute myelin water (expressed as milliliter of myelin water per milliliter of brain tissue) by referencing the myelin water signal to the signal of an external water standard attached to a subject's head (Whittall et al., 1997) or the signal of the CSF. The FAST-T2 sequence used in this work is being further modified to provide fast absolute myelin water mapping in clinically relevant scan time.

In conclusion, it is known that remyelination can occur within the adult central nervous system, however this mechanism fails to occur in a reliable manner in patients with multiple sclerosis, and factors contributing to this limited reparative response are not fully elucidated (Fancy et al., 2010). Understanding the potential for endogenous myelin repair among different subtypes of MS lesions is essential when considering the design of therapeutic clinical trials for remyelination. FAST-T2, is a feasible method to investigate specific patient and lesion characteristics that may contribute to differences in MWF recovery as well as to assess the potential benefit of a treatment intervention. Furthermore, we demonstrated that the majority of change occurs in the earliest stages after lesion development and that the intensity of the acute inflammatory event is detrimental on MWF recovery.

Disclosures of interest

Wendy S. Vargas has served on an advisory board for Teva Pharmaceuticals and received grant support from the National Multiple Sclerosis Society and Teva Pharmaceuticals.

Elizabeth Monohan, BS reports no disclosures.

Sneha Pandya, MS reports no disclosures.

Ashish Raj, PhD reports no disclosures.

Thanh D. Nguyen, PhD reports no disclosures.

Timothy Vartanian, MD, PhD is a speaker for Teva Neuroscience, has received honoraria for advising Genzyme, and has received grant support from the National Multiple Sclerosis Society, Biogen Idec, and Questcor.

Sandra M. Hurtado Rúa, PhD reports no disclosures.

Susan A. Gauthier DO, MPH has received honoraria for advising Genzyme and Teva Neuroscience and has received grant support from the National Multiple Sclerosis Society, Biogen Idec, Novartis Pharmaceuticals, Questcor, Genzyme, and EMD Serono.

Acknowledgments

We acknowledge the following clinicians: Dr. Jai Perumal, and Dr. Nancy Nealon. We further acknowledge the funding from the NMSS (RG 4661-A-2) and CTSC grant UL1 TR000457-06.

References

Bitsch, A., Kuhlmann, T., Da Costa, C., Bunkowski, S., Polak, T., Brück, W., 2000. Tumour necrosis factor alpha mRNA expression in early multiple sclerosis lesions: correlation with demyelinating activity and oligodendrocyte pathology. Glia 29 (4), 366–375. http://dx.doi.org/10.1002/(SICI)1098-1136(20000215)29:4<366::AID-GLIA7>3.0.CO;2-Y10652446.

Bland, J.M., Altman, D.G., 1999. Measuring agreement in method comparison studies. Stat. Methods Med. Res. 8 (2), 135–160. http://dx.doi.org/10.1191/096228099967381927210501650.

Blezer, E.L., Bauer, J., Brok, H.P., Nicolay, K., Hart, B.A., 2007. Quantitative MRI-pathology correlations of brain white matter lesions developing in a non-human primate model of multiple sclerosis. N.M.R. Biomed. 20 (2), 90–103. http://dx.doi.org/10.1002/nbm.108516948176.

Brown, R.A., Narayanan, S., Arnold, D.L., 2013. Segmentation of magnetization transfer ratio lesions for longitudinal analysis of demyelination and remyelination in multiple sclerosis. NeuroImage 66, 103–109. http://dx.doi.org/10.1016/j.neuroimage.2012.10.05923110887.

Chang, A., Tourtellotte, W.W., Rudick, R., Trapp, B.D., 2002. Premyelinating oligodendrocytes in chronic lesions of multiple sclerosis. N. Engl. J. Med. 346 (3), 165–173. http://dx.doi.org/10.1056/NEJMoa01099411796850.

Chen, J.T., Collins, D.L., Atkins, H.L., Freedman, M.S., Arnold, D.L., Canadian MS/BMT Study Group, 2008. Magnetization transfer ratio evolution with demyelination and remyelination in multiple sclerosis lesions. Ann. Neurol. 63 (2), 254–262. http://dx.doi.org/10.1002/ana.2130218257039.

Chen, J.T., Kuhlmann, T., Jansen, G.H., et al., 2007. Voxel-based analysis of the evolution of magnetization transfer ratio to quantify remyelination and demyelination with histopathological validation in a multiple sclerosis lesion. NeuroImage 36 (4), 1152–1158. http://dx.doi.org/10.1016/j.neuroimage.2007.03.07317543541.

Cotton, F., Weiner, H.L., Jolesz, F.A., Guttmann, C.R., 2003. MRI contrast uptake in new lesions in relapsing–remitting MS followed at weekly intervals. Neurol. 60 (4), 640–646. http://dx.doi.org/10.1212/01.WNL.0000046587.83503.1E12601106.

Deoni, S.C., Rutt, B.K., Arun, T., Pierpaoli, C., Jones, D.K., 2008. Gleaning multicomponent T1 and T2 information from steady-state imaging data. Magn Reson Med 60 (6), 1372–1387. http://dx.doi.org/10.1002/mrm.2170419025904.

Fancy, S.P., Kotter, M.R., Harrington, E.P., et al., 2010. Overcoming remyelination failure in multiple sclerosis and other myelin disorders. Exp. Neurol. 225 (1), 18–23. http://dx.doi.org/10.1016/j.expneurol.2009.12.02020044992.

Fischl, B., 2012. Freesurfer. NeuroImage 62 (2), 774–781. http://dx.doi.org/10.1016/j.neuroimage.2012.01.02122248573.

Franklin, R.J., 2002. Why does remyelination fail in multiple sclerosis? Nat. Rev. Neurosci. 3 (9), 705–714. http://dx.doi.org/10.1038/nrn91712209119.

Franklin, R.J., Ffrench-Constant, C., 2008. Remyelination in the CNS: from biology to therapy. Nat. Rev. Neurosci. 9 (11), 839–855. http://dx.doi.org/10.1038/nrn248018931697.

Gareau, P.J., Rutt, B.K., Karlik, S.J., Mitchell, J.R., 2000. Magnetization transfer and multicomponent T2 relaxation measurements with histopathologic correlation in an experimental model of MS. J. Magn. Reson. Imaging 11 (6), 586–595. http://dx.doi.org/10.1002/1522-2586(200006)11:6<586::AID-JMRI3>3.0.CO;2-V10862056.

Greve, D.N., Fischl, B., 2009. Accurate and robust brain image alignment using boundary-based registration. NeuroImage 48 (1), 63–72. http://dx.doi.org/10.1016/j.neuroimage.2009.06.06019573611.

Kolind, S., Matthews, L., Johansen-Berg, H., et al., 2012. Myelin water imaging reflects clinical variability in multiple sclerosis. NeuroImage 60 (1), 263–270. http://dx.doi.org/10.1016/j.neuroimage.2011.11.07022155325.

Kumar, D., Nguyen, T.D., Gauthier, S.A., Raj, A., 2012. Bayesian algorithm using spatial priors for multiexponential T2 relaxometry from multiecho spin echo MRI. Magn. Reson. Med. 68 (5), 1536–1543. http://dx.doi.org/10.1002/mrm.24170.

Lassmann, H., 2011. Review: the architecture of inflammatory demyelinating lesions: implications for studies on pathogenesis. Neuropathol. Appl. Neurobiol. 37 (7), 698–710. http://dx.doi.org/10.1111/j.1365-2990.2011.01189.x21696413.

Lassmann, H., 2014. Mechanisms of white matter damage in multiple sclerosis. Glia 62 (11), 1816–1830. http://dx.doi.org/10.1002/glia.2259724470325.

Laule, C., Kozlowski, P., Leung, E., Li, D.K., Mackay, A.L., Moore, G.R., 2008. Myelin water imaging of multiple sclerosis at 7 T: correlations with histopathology. NeuroImage 40 (4), 1575–1580. http://dx.doi.org/10.1016/j.neuroimage.2007.12.00818321730.

Laule, C., Leung, E., Lis, D.K., et al., 2006. Myelin water imaging in multiple sclerosis: quantitative correlations with histopathology. Mult. Scler. 12 (6), 747–753. http://dx.doi.org/10.1177/13524585060709281726300 2.

Laule, C., Vavasour, I.M., Kolind, S.H., et al., 2007. Magnetic resonance imaging of myelin. Neurotherapeutics 4 (3), 460–484. http://dx.doi.org/10.1016/j.nurt.2007.05.004.

Laule, C., Vavasour, I.M., Moore, G.R., et al., 2004. Water content and myelin water fraction in multiple sclerosis. A T2 relaxation study. J. Neurol. 251 (3), 284–293. http://dx.doi.org/10.1007/s00415-004-0306-615015007.

MacKay, A., Laule, C., Vavasour, I., Bjarnason, T., Kolind, S., Mädler, B., 2006. Insights into brain microstructure from the T2 distribution. Magn. Reson. Imaging 24 (4), 515–525. http://dx.doi.org/10.1016/j.mri.2005.12.03716677958.

Meyers, S.M., Laule, C., Vavasour, I.M., et al., 2009. Reproducibility of myelin water fraction analysis: a comparison of region of interest and voxel-based analysis methods. Magn. Reson. Imaging 27 (8), 1096–1103. http://dx.doi.org/10.1016/j.mri.2009.02.00119356875.

Meyers, S.M., Vavasour, I.M., Mädler, B., et al., 2013. Multicenter measurements of myelin water fraction and geometric mean T2: intra- and intersite reproducibility. J. Magn. Reson. Imaging 38 (6), 1445–1453. http://dx.doi.org/10.1002/jmri.2410623553991.

Neema, M., Goldberg-Zimring, D., Guss, Z.D., et al., 2009. 3 T MRI relaxometry detects T2 prolongation in the cerebral normal-appearing white matter in multiple sclerosis. NeuroImage 46 (3), 633–641. http://dx.doi.org/10.1016/j.neuroimage.2009.03.00119281850.

Nguyen, T.D., Wisnieff, C., Cooper, M.A., et al., 2012. T2 prep three-dimensional spiral imaging with efficient whole brain coverage for myelin water quantification at 1.5 tesla. Magn. Reson. Med. 67 (3), 614–621. http://dx.doi.org/10.1002/mrm.2412822344579.

Oh, J., Han, E.T., Lee, M.C., Nelson, S.J., Pelletier, D., 2007. Multislice brain myelin water fractions at 3 T in multiple sclerosis. J Neuroimaging 17 (2), 156–163. http://dx.doi.org/10.1111/j.1552-6569.2007.00098.x17441837.

Oh, J., Han, E.T., Pelletier, D., Nelson, S.J., 2006. Measurement of in vivo multi-component T2 relaxation times for brain tissue using multi-slice T2 prep at 1.5 and 3 T. Magn. Reson. Imaging 24 (1), 33–43. http://dx.doi.org/10.1016/j.mri.2005.10.01616410176.

Patani, R., Balaratnam, M., Vora, A., Reynolds, R., 2007. Remyelination can be extensive in multiple sclerosis despite a long disease course. Neuropathol. Appl. Neurobiol. 33 (3), 277–287. http://dx.doi.org/10.1111/j.1365-2990.2007.00805.x17442065.

Patrikios, P., Stadelmann, C., Kutzelnigg, A., et al., 2006. Remyelination is extensive in a subset of multiple sclerosis patients. Brain 129 (12), 3165–3172. http://dx.doi.org/10.1093/brain/awl21716921173.

Piaton, G., Gould, R.M., Lubetzki, C., 2010. Axon–oligodendrocyte interactions during developmental myelination, demyelination and repair. J. Neurochem. 114 (5), 1243–1260. http://dx.doi.org/10.1111/j.1471-4159.2010.06831.x20524961.

Polman, C.H., Reingold, S.C., Edan, G., et al., 2005. Diagnostic criteria for multiple sclerosis: 2005 revisions to the "McDonald criteria". Ann. Neurol. 58 (6), 840–846. http://dx.doi.org/10.1002/ana.2070316283615.

Prasloski, T., Rauscher, A., MacKay, A.L., et al., 2012. Rapid whole cerebrum myelin water imaging using a 3D GRASE sequence. NeuroImage 63 (1), 533–539. http://dx.doi.org/10.1016/j.neuroimage.2012.06.06422776448.

Prineas, J.W., Barnard, R.O., Kwon, E.E., Sharer, L.R., Cho, E.S., 1993. Multiple sclerosis: remyelination of nascent lesions. Ann. Neurol. 33 (2), 137–151. http://dx.doi.org/10.1002/ana.4103302038434875.

Raine, C.S., Wu, E., 1993. Multiple sclerosis: remyelination in acute lesions. J. Neuropathol. Exp. Neurol. 52 (3), 199–204. http://dx.doi.org/10.1097/00005072-199305000-000037684075.

Raj, A., Pandya, S., Shen, X., LoCastro, E., Nguyen, T.D., Gauthier, S.A., 2014. Multi-compartment T2 relaxometry using a spatially constrained multi-Gaussian model. PLOS One 9 (6), e98391. http://dx.doi.org/10.1371/journal.pone.009839124896833.

Reuter, M., Schmansky, N.J., Rosas, H.D., Fischl, B., 2012. Within-subject template estimation for unbiased longitudinal image analysis. NeuroImage 61 (4), 1402–1418. http://dx.doi.org/10.1016/j.neuroimage.2012.02.08422430496.

Smith, K.J., Lassmann, H., 2002. The role of nitric oxide in multiple sclerosis. Lancet Neurol. 1 (4), 232–241. http://dx.doi.org/10.1016/S1474-4422(02)00102-312849456.

Soellinger, M., Langkammer, C., Seifert-Held, T., Fazekas, F., Ropele, S., 2011. Fast bound pool fraction mapping using stimulated echoes. Magn Reson Med 66 (3), 717–724. http://dx.doi.org/10.1002/mrm.2284621437973.

van Waesberghe, J.H., Kamphorst, W., De Groot, C.J., et al., 1999. Axonal loss in multiple sclerosis lesions: magnetic resonance imaging insights into substrates of disability. Ann. Neurol. 46 (5), 747–75410553992.

Vavasour, I.M., Clark, C.M., Li, D.K., Mackay, A.L., 2006. Reproducibility and reliability of MR measurements in white matter: clinical implications. NeuroImage 32 (2), 637–642. http://dx.doi.org/10.1016/j.neuroimage.2006.03.03616677833.

Vavasour, I.M., Laule, C., Li, D.K., et al., 2009. Longitudinal changes in myelin water fraction in two MS patients with active disease. J. Neurol. Sci. 276 (1–2), 49–53. http://dx.doi.org/10.1016/j.jns.2008.08.02218822435.

Whittall, K.P., MacKay, A.L., Graeb, D.A., Nugent, R.A., Li, D.K., Paty, D.W., 1997. In vivo measurement of T2 distributions and water contents in normal human brain. Magn Reson Med 37 (1), 34–43. http://dx.doi.org/10.1002/mrm.19103701078978630.